# Partial Oxidation of Methane in Hollow-Fiber Membrane Reactors Based on Alkaline-Earth Metal-Free $CO_2$-Tolerant Oxide

**Yanying Wei**
School of Chemistry and Chemical Engineering, South China University of Technology, 510640, Guangzhou, China

Inst. of Physical Chemistry and Electrochemistry, Leibniz University of Hannover, Callinstrasse 3A 30167 Hannover, Germany

**Qing Liao, Zhong Li, and Haihui Wang**
School of Chemistry and Chemical Engineering, South China University of Technology, 510640, Guangzhou, China

**Armin Feldhoff and Juergen Caro**
Inst. of Physical Chemistry and Electrochemistry, Leibniz University of Hannover, Callinstrasse 3A 30167 Hannover, Germany

*DOI 10.1002/aic.14540*
*Published online July 5, 2014 in Wiley Online Library (wileyonlinelibrary.com)*

*The U-shaped alkaline-earth metal-free $CO_2$-stable oxide hollow-fiber membranes based on $(Pr_{0.9}La_{0.1})_2(Ni_{0.74}Cu_{0.21}Ga_{0.05})O_{4+\delta}$ (PLNCG) are prepared by a phase-inversion spinning process and applied successfully in the partial oxidation of methane (POM) to syngas. The effects of temperature, $CH_4$ concentration and flow rate of the feed air on $CH_4$ conversion, CO selectivity, $H_2$/CO ratio, and oxygen permeation flux through the PLNCG hollow-fiber membrane are investigated in detail. The oxygen permeation flux arrives at approximately 10.5 mL/min cm$^2$ and the CO selectivity is higher than 99.5% with a $CH_4$ conversion of 97.0% and a $H_2$/CO ratio of 1.8 during 140 h steady operation. The spent hollow-fiber membrane still maintains a dense microstructure and the Ruddlesden-Popper $K_2NiF_4$-type structure, which indicates that the U-shaped alkaline-earth metal-free $CO_2$-tolerant PLNCG hollow-fiber membrane reactor can be steadily operated for POM to syngas with good performance.* © 2014 American Institute of Chemical Engineers *AIChE J*, 60: 3587–3595, 2014
*Keywords: membrane separations, oxygen permeation, hollow fiber, partial oxidation of methane, $CO_2$*

## Introduction

The economic use of natural gas has attracted extensive attention worldwide.[1] At present, natural gas is mainly converted into syngas ($CO + 2H_2$) by steam reforming. In a second step, a series of important chemical products such as liquid Fischer–Tropsch (F–T) fuels and methanol can be produced from syngas.[2] As a promising alternative for syngas generation, the catalytic partial oxidation of methane [POM, $CH_4 + 1/2O_2 \rightarrow CO + 2H_2$, $\Delta H$ (25°C) = −36 kJ/mol] has attracted increasing attention in recent years.[3] POM to syngas is a weakly exothermic reaction, and the reaction rate is 1–2 orders of magnitudes faster than that of steam reforming. Furthermore, the $H_2$/CO ratio is 2:1, which is a perfect stoichiometry for F–T and methanol syntheses. However, the downstream process requirements cannot tolerate nitrogen as ballast, that is, pure oxygen is required for POM. The investment cost in a cryogenic oxygen plant may cover 45% of the total investment cost of a POM to syngas plant.[4] An alternative route following the concept of process intensification is the use of a mixed oxygen-ionic and electronic conducting (MIEC) membrane[5–7] for the *in situ* oxygen separation from air combined with the catalytic POM in one device called catalytic membrane reactor.

To date, numerous studies have reported the development and application of MIEC membrane reactors in the POM to syngas, and the corresponding membrane materials, mainly perovskites, have been extensively investigated. Perovskites show a relatively high oxygen permeation flux compared with other oxygen-conducting oxides but their stability transpired to be a critical problem.[8–15] A chemical decomposition to $SrCO_3$ was observed on the $SrCo_{0.8}Fe_{0.2}O_{3-\delta}$ membrane reactor in syngas generation experiments.[16] Bouwmeester[13] also reported the formation of $SrCO_3$ on the membrane surface of $La_{0.6}Sr_{0.4}Co_{0.2}Fe_{0.8}O_{3-\delta}$ after POM operation for 3 days at 830°C. A $BaCo_xFe_yZr_zO_{3-\delta}$ hollow-fiber membrane reactor coated with catalyst survived only 5 h in the POM.[17] From the concept of "oxidation-reforming" mechanism for POM, the high $CO_2$-concentration from the methane total oxidation to $CO_2$ and $H_2O$ near the membrane surface results in the formation of alkaline-earth metal carbonates. Caro et al.[18] and Kleinert et al.[19] also noted that the failure of the hollow-fiber membrane applied in POM was due to the formation of carbonate. In sum, most of the

Correspondence concerning this article should be addressed to H. H. Wang at hhwang@scut.edu.cn.

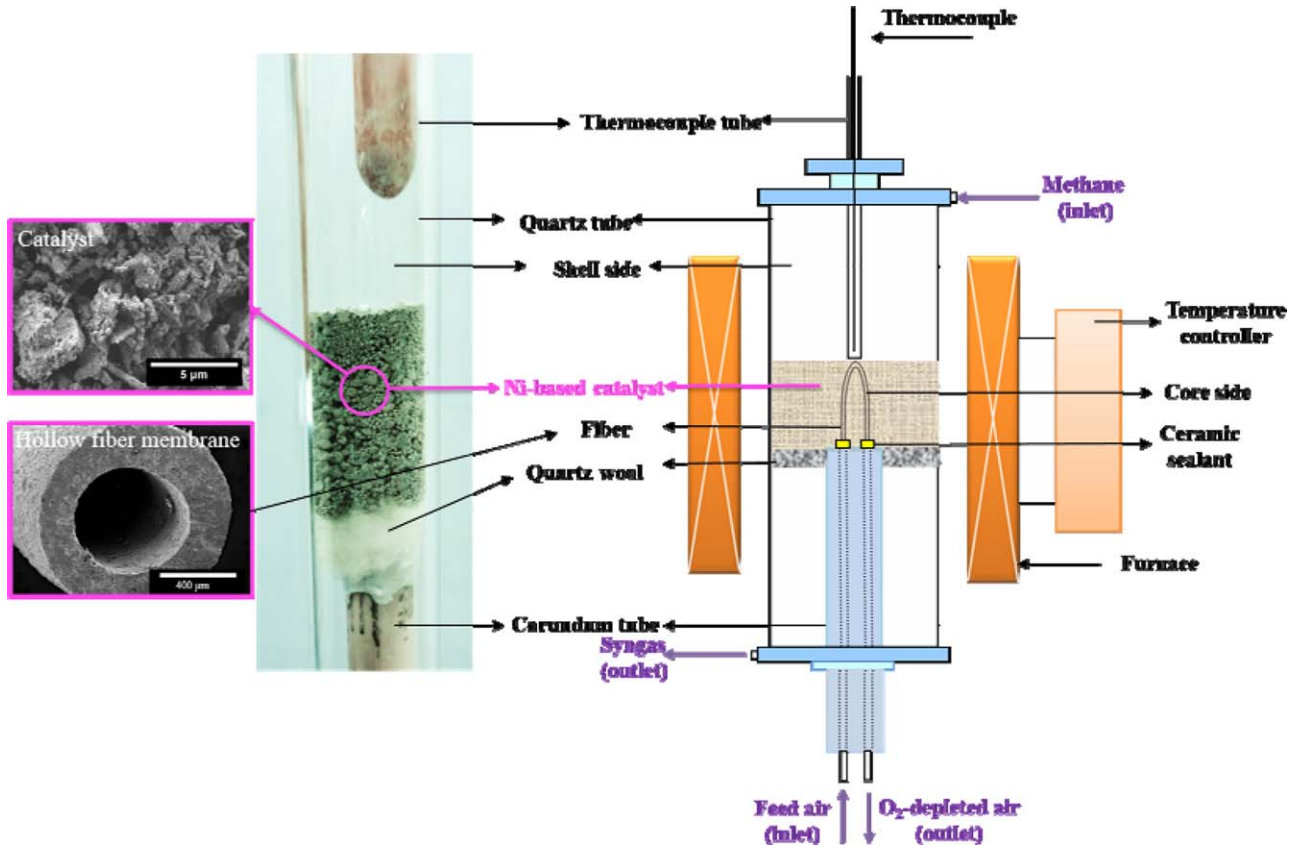


**Figure 1. Configuration of the U-shaped PLNCG hollow-fiber membrane reactor for POM.**

**[Color figure can be viewed in the online issue, which is available at wileyonlinelibrary.com.]**

perovskites contain the alkaline-earth metal elements, which tend to react with $CO_2$ under POM conditions and form carbonates, although a proper membrane reactor operation can prevent the further decomposition of a perovskite membrane in the reducing atmosphere of a POM.[20] The instability of alkaline-earth metal-containing materials will lead to the failure of a membrane reactor in the POM. Therefore, alkaline-earth metal-free $CO_2$-tolerant MIEC membranes with better stability will be a good choice for POM.

In recent years, intensive efforts have been made to develop $CO_2$-tolerant oxygen permeable membrane materials.[21,22] A Ruddlesden-Popper $K_2NiF_4$-type phase of the composition $(Pr_{0.9}La_{0.1})_2(Ni_{0.74}Cu_{0.21}Ga_{0.05})O_{4+\delta}$ (PLNCG), which developed by Yashima et al.,[23] was also found to exhibit good oxygen permeability and good resistance to $CO_2$ in our previous work.[24,25] However, only a few applications in the POM to syngas with these $CO_2$-tolerant materials have been published so far. Therefore, in this article, a membrane reactor based on the alkaline-earth metal-free $CO_2$-stable $K_2NiF_4$-type oxide PLNCG will be used for coupling the *in situ* oxygen separation from air and the POM to syngas. It has been reported that the reactor with smaller diameter ($D$) and greater length-to-diameter ratio ($L/D$) gives better performance in terms of high $CH_4$ conversion in POM.[26] The hollow-fiber membranes exhibit many advantages, such as the large membrane area per unit volume for oxygen permeation, high oxygen permeation flux, easy assembly for large-scale module fabrications. Furthermore, the specific U-shaped hollow-fiber geometry can avoid the breakage of the membrane due to the expansion or shrinkage at changing temperatures.[27] Therefore, the U-shaped PLNCG hollow-fiber membranes are chosen in this study.

## Experimental

Powders of PLNCG, $Ba_{0.5}Sr_{0.5}Co_{0.8}Fe_{0.2}O_{3-\delta}$ (BSCF), and $BaCo_{0.4}Fe_{0.4}Zr_{0.2}O_{3-\delta}$ (BCFZ) were prepared through the sol-gel route[24] and the U-shaped PLNCG hollow fibers were fabricated through a phase-inversion spinning process, which can be found in our previous work.[28] The as-prepared PLNCG, BSCF, and BCFZ powders were treated in various atmospheres at 900°C for different time. The powder samples before and after gas treatment, as well as the fresh and spent PLNCG hollow-fiber membranes were characterized by X-ray diffraction (XRD, Bruker-D8 ADVANCE, Cu-K$\alpha$ radiation). The microstructure and morphology of the fresh and spent PLNCG hollow-fiber were observed by a scanning electron microscope (SEM, JEOL JSM-6490LA) with energy dispersive X-ray spectrometer (EDXS).

The POM in the U-shaped PLNCG hollow-fiber membrane reactor was investigated in a high-temperature permeation cell, as shown in Figure 1. The Ni-based catalyst (an commercial steam reforming catalyst of Süd Chemie AG, now Clariant, BET surface area is 170–200 $m^2/g$, Ni: 42.7 wt %, Al: 14.1 wt %, Si: 5 wt %) was packed around the whole U-shaped hollow-fiber membrane above the quartz wool as support. The particle size of catalyst was between 0.2 and 0.4 mm, catalyst was diluted with silica of the same grain size (catalyst mass ≈60%) and the catalytic bed height was near 3 cm. The distance between the thermocouple and the catalytic bed was about 5 mm to ensure a more or less accurate temperature control. As the POM reaction is a weakly exothermic reaction, it cannot be excluded that the real temperature was slightly higher than detected. However, under most of our experimental conditions, methane was

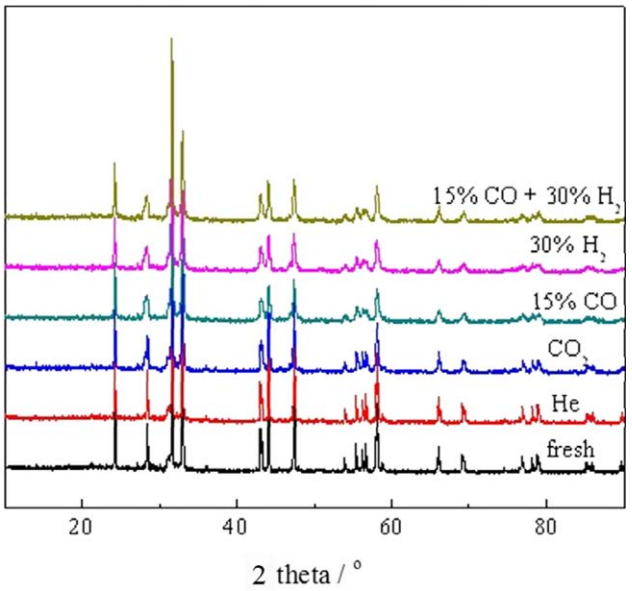


**Figure 2. XRD patterns of the PLNCG powder before and after exposure to various atmospheres at 900°C for 1 h.**

**[Color figure can be viewed in the online issue, which is available at wileyonlinelibrary.com.]**

diluted with helium, which makes it easier to keep a constant reactor temperature. Therefore, the detected temperature seems to represent the real temperature within ±10°C. Air was fed to the core side while $CH_4$ or a mixture of He and $CH_4$ was fed to the shell side. Composition of the outlet gases was measured using an online coupled gas chromatograph (GC, Agilent 7890) with a thermal conductivity detector (TCD). $CH_4$ conversion ($X_{CH4}$), CO selectivity ($S_{CO}$), and oxygen permeation flux ($J_{O2}$) can be calculated through hydrogen balance and oxygen balance, which can be defined as follows

$$X_{CH_4} = \frac{F^{in}_{CH_4} - F^{out}_{CH_4}}{F^{in}_{CH_4}} \quad (1)$$

$$S_{CO} = \frac{F_{CO}}{F_{CO} + F_{CO_2}} \quad (2)$$

$$J_{O_2} = \frac{F_{CO} + 2F_{CO_2} + F_{H_2O} + 2F_{O_2}(\text{unreacted})}{2S} \quad (3)$$

where $F_{gas}$ is the flow rate of the corresponding gas, superscript of "in" and "out" is the gas direction, and $S$ is the effective hollow-fiber membrane area.

## Results and Discussion

### *Powder stability under syngas condition*

It is very important to test the stability of PLNCG under POM reaction conditions, that is, CO and $H_2$ containing atmosphere, even though it is stable in $CO_2$.[24,25]. Therefore, PLNCG powder was treated in various atmospheres at 900°C for 1 h, including He, $CO_2$, 15% CO balanced with He, 30% $H_2$ balanced with He, and syngas (15% CO + 30% $H_2$) balanced with He, which is shown in Figure 2. It can be found that PLNCG still keeps its $K_2NiF_4$-type structure under CO and $H_2$ atmosphere. To confirm the earlier statement, PLNCG powder was treated for different exposure times in a syngas atmosphere (15% CO + 30% $H_2$). The phase structures of PLNCG for the exposure time of 1, 5, and 12 h are shown in Figure 3. Compared with the fresh powder, the PLNCG powder exposed to syngas for even 12 h still exhibits the $K_2NiF_4$-type structure.

Conversely, BSCF and BCFZ were also chosen for comparision. As one of the most popular mixed conducting oxide with excellent oxygen permeability,[29,30] BSCF seems to be not stable enough in syngas atmosphere. As shown in Figure 4a, after exposure to syngas at 900°C for 1 h, the material of BSCF decomposes and new reflections of $BaCO_3$, BaO, CoO, $Co_3O_4$ appear in the XRD pattern. As a much more stable mixed conducting oxide,[31] which can be applied in POM steadily for more than 2000 h,[32] BCFZ can maintain the primary reflections of the perovskite structure unchanged after syngas treatment, as shown in Figure 4b. However, some other phases of $BaCO_3$ and $Co_3O_4$ are formed. Table 1 summarizes the stability and decomposition products, respectively, of PLNCG, BSCF, and BCFZ powders after exposure to various atmospheres at 900°C for 1 h. Compared with BSCF and BCFZ, PLNCG shows much better chemical and phase stability under these harsh atmospheres. In other words, PLNCG is stable not only in $CO_2$ but also in CO and $H_2$ containing atmospheres (POM conditions). Therefore, with the expectation of a good stability, PLNCG hollow-fiber membranes were applied in POM in the following work.

### *Effect of different operation conditions on POM performance*

The time dependence of the oxygen permeation flux and the catalytic performance of the U-shaped PLNCG hollow-fiber membrane during the initial stage of POM are shown in Figure 5. The $CH_4$ conversion keeps constant at 100% in the first 20 h. In this period, the oxygen permeation flux through the membrane slightly increases from 11.2 to 11.8 mL/min $cm^2$, while the CO selectivity decreases from

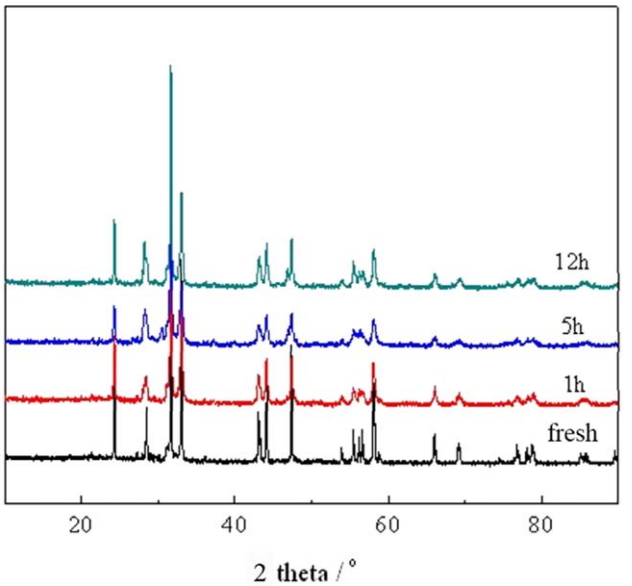


**Figure 3. XRD patterns of the PLNCG powder before and after exposure to syngas for different exposure time at 900°C.**

**[Color figure can be viewed in the online issue, which is available at wileyonlinelibrary.com.]**

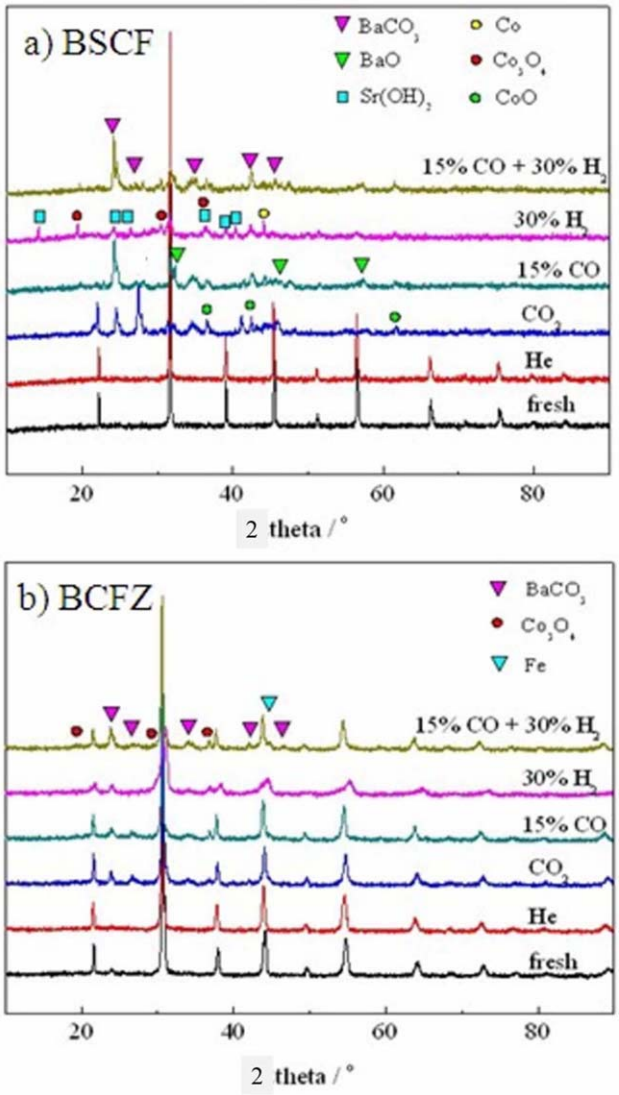


**Figure 4. XRD patterns of the (a) BSCF and (b) BCFZ powder before and after exposure to various atmospheres at 900°C for 1 h.**

**[Color figure can be viewed in the online issue, which is available at wileyonlinelibrary.com.]**

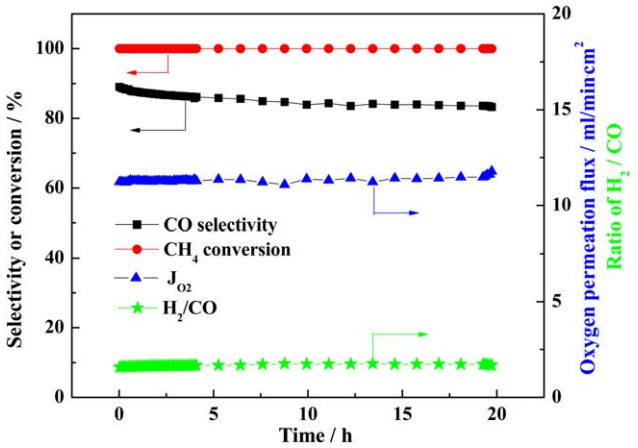


**Figure 5. Time dependence of the $CH_4$ conversion, CO selectivity, $H_2$/CO ratio, and the oxygen permeation flux of the U-shaped PLNCG hollow-fiber membrane during the initial stage of POM.**

**Conditions: $T = 950$°C, $F_{air} = 110$ mL/min, $F_{He+CH4} = 60$ mL/min, $C_{CH4} = 20.3\%$. [Color figure can be viewed in the online issue, which is available at wileyonlinelibrary.com.]**

89% to 83%. Over this 20 h operation, the $H_2$/CO ratio was found to be 1.7. The missing hydrogen is attributed to the deep oxidation to $H_2O$ while CO keeps at a relatively high selectivity. It can be found that it took only a short time for the membrane reactor to achieve a steady state from Figure 5. The performance in the initial stage is related to the reduction rate of the Ni-based catalyst which has been also found in other studies on POM in membrane reactors.[33–35] Dong et al.[33] showed that the initial catalyst was reduced from the oxidation state of NiO to $Ni^0$ starting from the outer layer of the catalysts to the center gradually, and as a result, the catalytic performance of the catalyst was improved also gradually. Tsai et al.[10] found that the oxygen permetion rate increased very slowly and reached its steady state after 500 h in a dense disk-shaped $La_{0.2}Ba_{0.8}Co_{0.2}Fe_{0.8}O_{3-\delta}$ membrane reactor in the POM reaction. But almost 21 h were needed for the BSCF disk-shaped membrane reactor to reach its steady state.[33] In other words, the initial stage of membrane reactors based on different materials will be different, which might be related to the adjustment between the membrane and the new environment. However, a shorter initial time for POM was obtained in a tubular BSCF membrane reactor and only 1 h was needed to reach the steady state, which demonstrates that the initial stage is also affected by the membrane configuration.[36] However, in our case during this initial stage in the PLNCG hollow-fiber membrane reactor, no sharp increase or decrease of the oxygen permeation flux, $CH_4$ conversion, or CO selectivity are observed. In addition, a probable reason for this experimental finding seems to be that the relative high operation temperature accelerates the reduction rate of the catalyst and shortens the activation time, which is also in according with Li's finding.[34] Therefore, the initial reaction process of the membrane reactor for POM is closely dependent on the membrane reactor configuration, feeding mode, methane partial pressure, membrane material, and the activation ability of the catalyst.[35] After reaching the steady state, the effects of operation temperature, flow rate of $CH_4$ and air on the POM reaction are investigated to understand the catalytic performance of our PLNCG hollow-fiber membrane reactor and find the best and economical operation conditions for such a membrane reactor in POM.

**Table 1. Stability and Decomposition Products, Respectively, of Different Oxygen Permeable Membrane Materials in Various Atmospheres (900°C, 1 h)**

| | He | $CO_2$ | 15% CO | 30% $H_2$ | syngas (15%CO + 30%$H_2$) |
|---|---|---|---|---|---|
| PLNCG | Stable | Stable | Stable | Stable | Stable |
| BSCF | Stable | $BaCO_3$, CoO | $BaCO_3$, BaO, CoO | $Sr(OH)_2$, $Co_3O_4$, Co | $BaCO_3$, BaO, CoO, $Co_3O_4$ |
| BCFZ | Stable | $BaCO_3$, $Co_3O_4$ | $BaCO_3$, $Co_3O_4$ | $Co_3O_4$, Fe | $BaCO_3$, $Co_3O_4$, Fe |

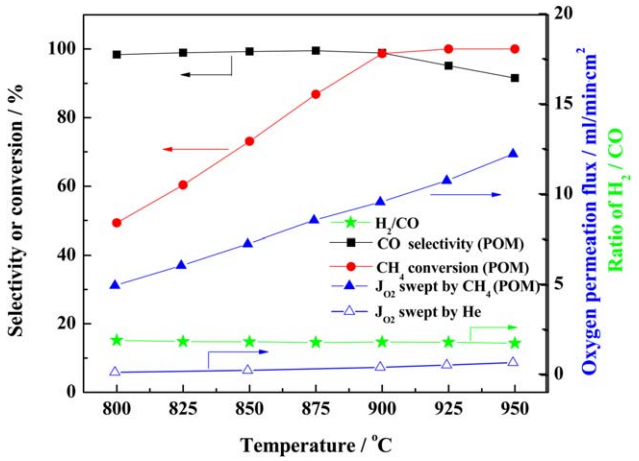


**Figure 6. Temperature dependence of the $CH_4$ conversion, CO selectivity, $H_2$/CO ratio, oxygen permeation flux swept by $CH_4$ in POM and that swept by He.**

**Conditions: $F_{air} = 110$ mL/min, $F_{He(+CH4)} = 60$ mL/min, $C_{CH4} = 25.9\%$ in POM. [Color figure can be viewed in the online issue, which is available at wileyonlinelibrary.com.]**

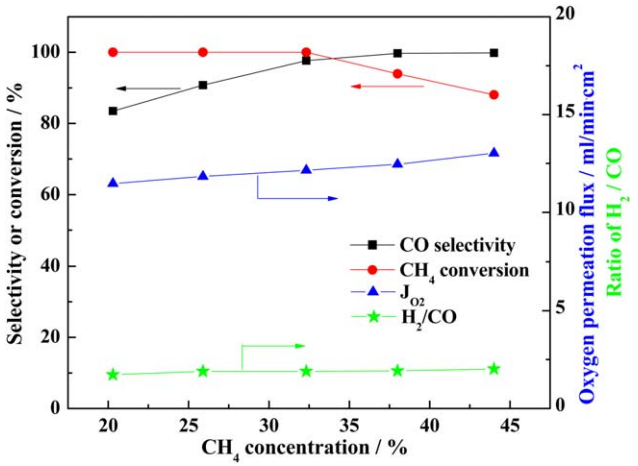


**Figure 7. Influence of methane concentration in the reaction side on the $CH_4$ conversion, CO selectivity, $H_2$/CO ratio, and the oxygen permeation flux in POM.**

**Conditions: $T = 950$°C, $F_{air} = 110$ mL/min, $F_{He+CH4} = 60$ mL/min. [Color figure can be viewed in the online issue, which is available at wileyonlinelibrary.com.]**

Figure 6 shows the temperature dependence of $CH_4$ conversion, CO selectivity, oxygen permeation flux, and $H_2$/CO ratio. It can be seen that the $CH_4$ conversion increases from 50% to 100%, and the oxygen permeation flux increases from 4.9 to 12.2 mL/min cm$^2$ with increasing temperatures from 800 to 950°C, while the CO selectivity decreases from 98% to 92% and the $H_2$/CO ratio keeps around 2. The increase of the oxygen permeation flux is due to the increase of the oxygen diffusion rate through the oxygen membrane and an enhanced surface exchange rate with increasing temperatures, which is in complete accordance with the conclusions in our previous work.[28] Resulting from the increase of the oxygen permeation flux, the methane conversion increases because it is mainly controlled by the amount of the permeated oxygen. When the amount of the oxygen in the $CH_4$ side is more than the needed amount for the stoichiometric POM, the CO selectivity decreases due to the deeper oxidation of CO with increasing temperature. As presented in Figure 6, the oxygen permeation flux through the U-shaped PLNCG hollow-fiber membrane under the oxygen partial pressure gradient of air/$CH_4$ with Ni-based catalyst is an order of magnitude higher than that under an air/He gradient. Because the permeated oxygen prefers to react with $CH_4$ quickly, the oxygen partial pressure gradient in POM membrane reactors is much larger than that under conventional permeation conditions using nonreactive sweep gases. Yang and coworkers[36] also compared the oxygen permeation flux under the POM reaction condition with that when using helium as sweep gas. They found that the presence of methane in the BSCF tubular membrane could lower the oxygen partial pressure deeply and the oxygen permeation flux was enhanced by 8–10 times. Li et al.[34] also found that the oxygen permeation flux increased eightfold in the presence of a catalyst in the $BaCe_{0.1}Co_{0.4}Fe_{0.5}O_{3-\delta}$ membrane reactor for POM.

Figure 7 shows the influence of the methane concentration on the performance of the POM membrane reactor. The different methane concentrations are obtained by adjusting the ratio of methane and helium. As shown in Figure 7, with increasing methane concentration, the $CH_4$ conversion first keeps 100% since enough oxygen is available, but then the $CH_4$ conversion begins to decrease once the methane concentration is higher than 32%, which can be ascribed to the high $CH_4/O_2$ ratio. On the contrary, the CO selectivity and the oxygen permeation flux increase with increasing methane concentration. A higher methane concentration means a higher partial pressure of methane, which leads to a biger oxygen partial pressure gradient as the driving force over the membrane. Therefore, the oxygen permeation flux increases as the methane concentration increases. However, the $CH_4/O_2$ ratio increases and as a result, a higher CO selectivity can be obtained at a higher methane concentration because the partial oxidation to produce CO is favored. In Figure 8, the effect of the methane flow rate on the POM performance is also investigated. Different from the conditions in Figure 7 where the He-diluted $CH_4$ is used, here we applied pure $CH_4$ as reactant. The CO selectivity and the oxygen permeation flux increase while the $CH_4$ conversion decreases with increasing $CH_4$ flow rate. Under such reaction condition with a high methane flow rate, the permeated oxygen is not enough to completely consume the fed methane. As a result, the $CH_4$ conversion decreases and the CO selectivity increases with increasing methane flow rate. In both Figures 7 and 8, the $H_2$/CO ratio is around 2.

For the other side of the membrane reactor, the effect of the air flow rate on the performance of the POM membrane reactor is plotted in Figure 9. The $CH_4$ conversion keeps 100% for all air flow rates, which indicates that there is enough oxygen permeated through the membrane to consume the methane completely. With increasing air flow rate, the oxygen permeation flux increases while the CO selectivity decreases, but this trend is very slight. Compared to the effect of the methane flow rate on the performance of the PLNCG hollow-fiber membrane reactor, the influence of the air flow rate is less remarkable. For the $BaCe_{0.1}Co_{0.4}Fe_{0.5}O_{3-\delta}$ POM membrane reactor, a similar phenomenon was also found by Li et al.[34]

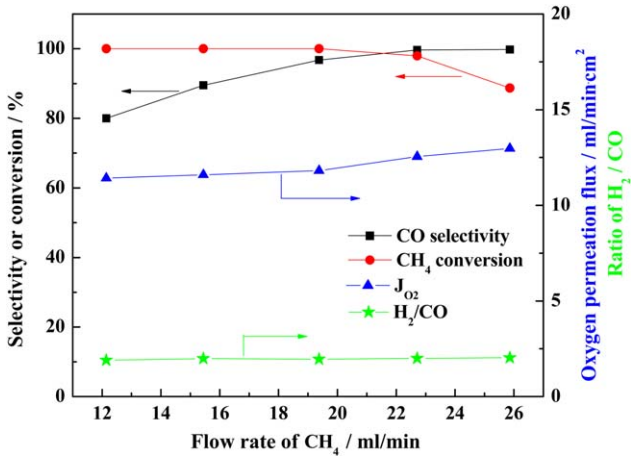


**Figure 8. Effect of the methane flow rate in the reaction side on the $CH_4$ conversion, CO selectivity, $H_2$/CO ratio and the oxygen permeation flux in POM.**

**Conditions: $T = 950°C$, $F_{air} = 110$ mL/min, $C_{CH4} = 100\%$. [Color figure can be viewed in the online issue, which is available at wileyonlinelibrary.com.]**

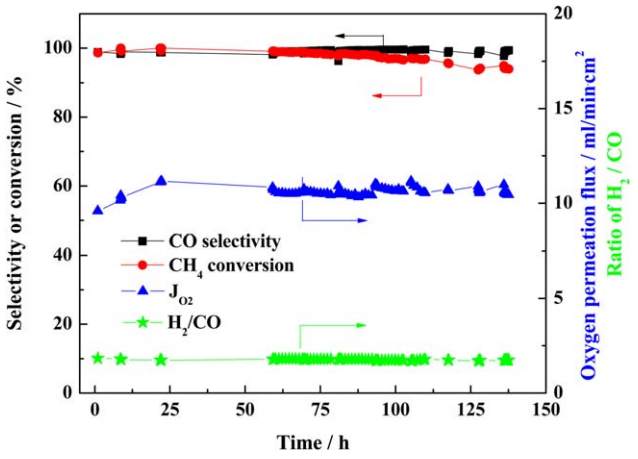


**Figure 10. Time dependence of $CH_4$ conversion, CO selectivity, $H_2$/CO ratio and $J_{O2}$ in POM reaction in the U-shaped hollow-fiber membrane.**

**Conditions: $T = 900°C$, $F_{air} = 110$ mL/min, $F_{He+CH4} = 60$ mL/min, $C_{CH4} = 25.9\%$. [Color figure can be viewed in the online issue, which is available at wileyonlinelibrary.com.]**

### *Stability of PLNCG hollow-fiber membrane in POM*

The stability of a membrane reactor is very important for its practical application in POM. In recent decades, the lifetime of the membrane reactor has been prolonged by different methods, such as developing new materials which are stable under the POM reaction conditions;[33,37] modifying the operation mode by adding a small amount of oxygen into the methane[38]; precise temperature controlling by correct monitoring of the heat system in the POM process.[39] For the disk-membrane reactor based on $BaCe_{0.1}Co_{0.4}Fe_{0.5}O_{3-\delta}$, a 1000 h continuous operation of POM was performed without any decrease of $CH_4$ conversion, CO selectivity and oxygen permeation flux.[34] For the tubular membrane reactor based on $La_{0.5}Sr_{0.5}FeO_{3-\delta}$, the long-term test showed stable performance during more than 7000 h with the $CH_4$ conversion and CO selectivity of not less than 98.8% and 90%, respectively.[39] For the disk-type and tubular membrane reactors, the lifetime can reach several hundreds or even thousands of hours under POM conditions. However, there is only a few literature about the long-term operation in hollow-fiber membrane reactors for POM. Because there are many factors which will block the POM reaction in hollow-fiber membrane reactors, such as material's instability under reducing atmosphere, carbonate formation,[40] solid state reaction between catalyst and membrane,[17] coke deposition,[18,19] and so forth. Therefore, the long-term operation of hollow-fiber membrane reactors in POM is reported rarely, and until now, only Caro et al.[41] reported the 300 h long-term study in

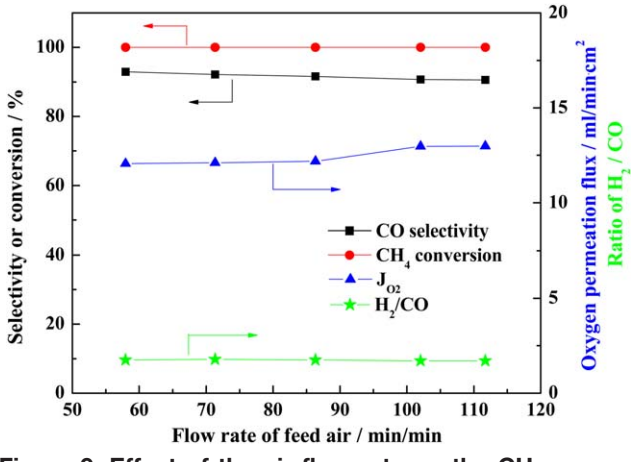


**Figure 9. Effect of the air flow rate on the $CH_4$ conversion, CO selectivity, $H_2$/CO ratio, and the oxygen permeation flux in POM.**

**Conditions: $T = 950°C$, $F_{He+CH4} = 60$ mL/min, $C_{CH4} = 25.9\%$. [Color figure can be viewed in the online issue, which is available at wileyonlinelibrary.com.]**

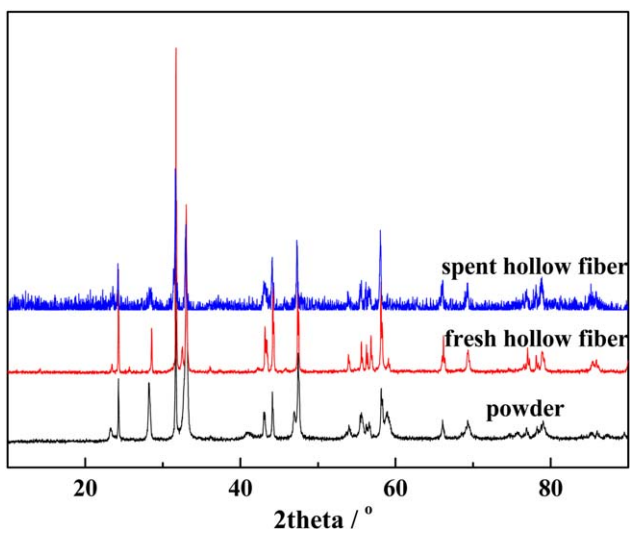


**Figure 11. XRD patterns of the PLNCG powder, fresh and spent hollow-fiber membrane after 140 h operation in the POM to syngas (for the experimental details see Figure 10).**

**[Color figure can be viewed in the online issue, which is available at wileyonlinelibrary.com.]**

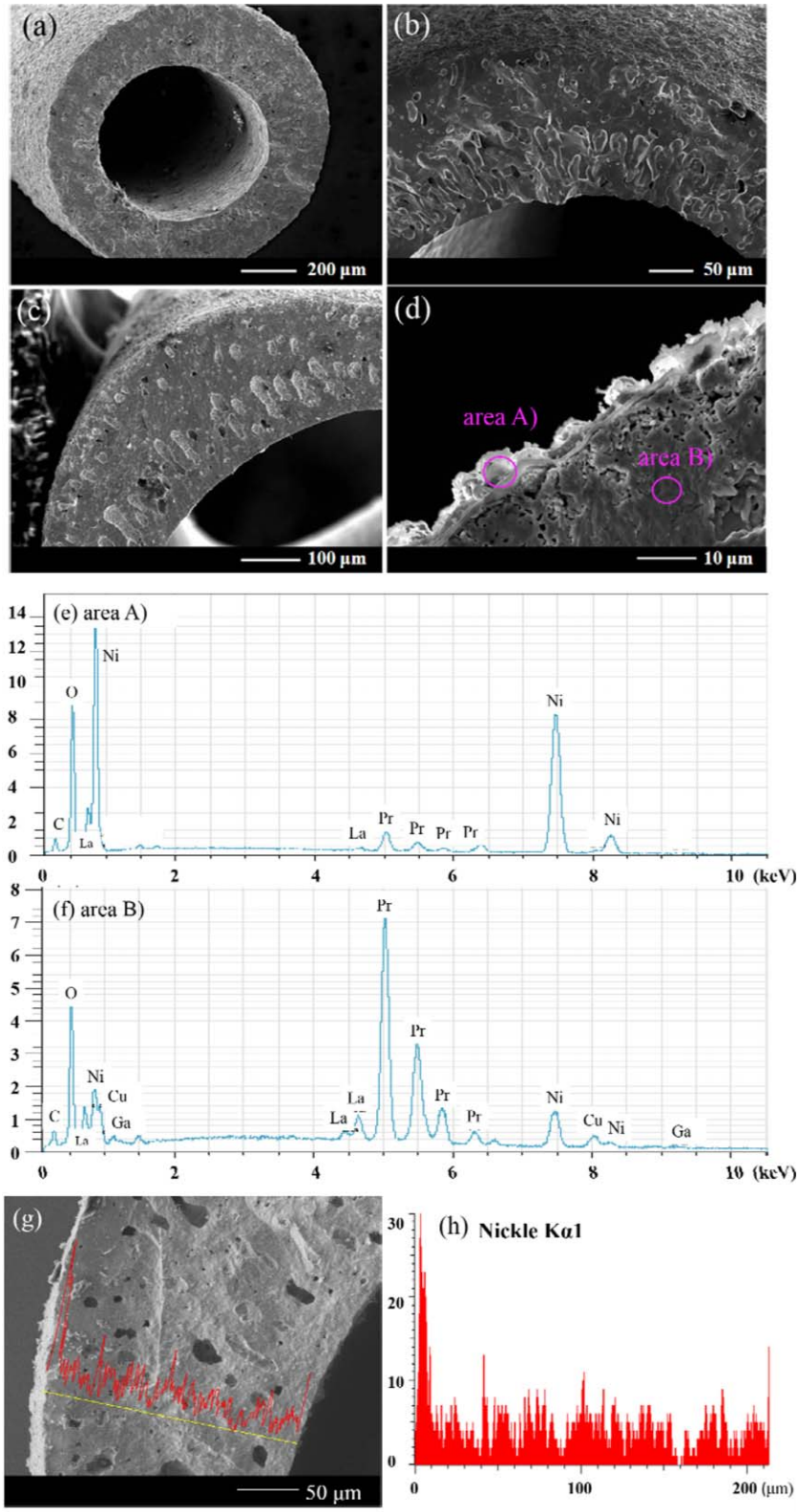


**Figure 12. SEM micrographs of the cross-section of the fresh PLNCG hollow-fiber membrane (a and b); and that of the spent hollow-fiber membrane (c and d). (d) shows a cross-section area near to the outer surface of the hollow-fiber membrane which was in direct contact with the Ni catalyst. (e and f) show the EDX spectra of areas A and B as marked in (d). (g and h) show the Ni-Kα line scan of the spent membrane.**

**[Color figure can be viewed in the online issue, which is available at wileyonlinelibrary.com.]**

$BaCo_xFe_yZr_zO_{3-\delta}$ hollow-fiber membrane reactor for POM. In their study, the catalyst was separated from the hollow-fiber membrane by a porous tube, and steam was added into methane to avoid coke deposition. Turning back to our work, it has to be pointed out that our membrane is in direct contact with the catalyst and no steam is added to the

methane feed. More than 140-hour continuous operation of POM is performed at 900°C in such a U-shaped alkaline-earth metal-free $CO_2$-tolerant PLNCG hollow-fiber membrane reactor. As shown in Figure 10, the oxygen permeation flux reaches approximately 10.5 mL/min $cm^2$ and the CO selectivity is higher than 99.5% while the $CH_4$ conversion is around 97.0%, the $H_2$/CO ratio is about 2, exactly 1.8, the missing $H_2$ is due to the deep oxidation to $H_2O$. Over the 140 h operation, the performance of the PLNCG hollow-fiber membrane reactor remains stable with an only slightly decrease of the $CH_4$ conversion after 100 h, which is related to coke deposition. There are different methods to avoid coke formation. Using methane/steam mixtures as feed with $CH_4/H_2O \leq 1$ allows to conduct the POM without coke deposition on the Ni-based catalyst.[18,19] The coke deposition could also be slowed down by cofeeding $CH_4$ and $CO_2$ as feed due to the Boudouard reaction between $CO_2$ and coke.[42–44] Efforts of avoiding the coke formation on the catalyst to extend the lifetime of PLNCG hollow-fiber membrane reactor for POM are under study. However, compared with other hollow-fiber oxygen permeable membrane reactors for POM, the PLNCG hollow-fiber membrane exhibits a good reaction performance and promising stability.

### *Characterization of the spent membrane*

After 140 h steady POM operation, the PLNCG hollow-fiber membrane was still gastight. The spent membrane was characterized by XRD, SEM, and EDXS. Figure 11 presents the XRD phase structures of the starting PLNCG powder, the fresh and spent hollow-fiber membranes after 140 h operation in the POM. The XRD patterns indicate that all materials are pure $K_2NiF_4$-structures. Furthermore, after 140 h operation time, no carbonates or other new phases are observed. Although the XRD pattern alone cannot sufficiently prove the stability of the membrane because only the crystalline phases in a concentration higher than 5% can be detected, XRD is a helpful analytical tool to prove chemical as well as phase stability.

Figures 12a, b show the SEM micrographs of the cross-section of the fresh PLNCG hollow-fiber membrane. Finger-like structures can be observed in the wall of PLNCG hollow-fiber membrane near the inner surface, which is beneficial for improving the surface exchange rate during POM. Figures 12c, d show the cross section of the spent hollow-fiber membrane and the wall part near the outer surface which was in direct contact to the Ni-based catalyst. It can be seen that the spent membrane maintains its compact structure. However, there are some μm-sized deposits on the outer surface of the membrane (Figure 12d). The EDX spectra of area A on the outer surface and area B in the membrane bulk in Figure 12d are shown in Figures 12e, f. From the EDX spectrum of area A (Figure 12e), a Ni enrichment on the surface is clearly indicated. The Ni signal at 0.85 keV stands for the electron transition L$\alpha$, the x-ray line at 7.5 keV reflects the K$\alpha$ transition. This Ni-enriched layer could stem (a) from the Ni-containing catalyst or (b) from the membrane by demixing and segregation. From the Ni EDXS line scan across the membrane (Figures 12g, h, using the Ni-K$\alpha$1 electron transition), we can learn that there is no Ni depletion in the bulk near to the surface of the PLNCG. In can be concluded, therefore, that the detected Ni enriched surface layer originates from the intimate contact of Ni catalyst and membrane (cf. Figure 1). It is reported in literature that a $BaCo_xFe_yZr_zO_{3-\delta}$ hollow-fiber membrane reactor failed after 9 h operation and the defect occurred at a position where the membrane was in direct contact with the Ni-based catalyst.[17] However, the Ni transfer in a solid state reaction on the outer membrane surface resulting from the intimate contact with the catalyst showed little negative effect on the membrane performance from our long-term operation in the POM in Figure 10.

All these above results demostrate that the U-shaped PLNCG hollow-fiber membrane reactor can be steadily operated in POM. Furthermore, such a hollow-fiber membrane reactor based on the alkaline-earth metal-free $CO_2$-tolerant material like PLNCG, exhibits a long lifetime among various hollow-fiber membrane reactors for POM with good reaction performance.

## Conclusions

The U-shaped alkaline-earth metal-free $CO_2$-tolerant PLNCG oxide hollow-fiber membranes were successfully prepared by a phase-inversion spinning process and evaluated in the POM to syngas. With increasing temperatures, the $CH_4$ conversion and the oxygen permeation flux increase, while the CO selectivity decreases. With increasing $CH_4$ concentration or $CH_4$ flow rate, the CO selectivity and the oxygen permeation flux increase while the $CH_4$ conversion decreases. The oxygen permeation flux through the U-shaped PLNCG hollow-fiber membrane under an oxygen partial pressure gradient of air/$CH_4$ is an order of magnitude higher than that under an air/He gradient at 950°C. More than 140 h steady POM operation is performed at 900°C in such a U-shaped alkaline-earth metal-free $CO_2$-stable PLNCG hollow-fiber membrane reactor with the oxygen permeation flux of 10.5 mL/min $cm^2$, CO selectivity of 99.5%, $CH_4$ conversion of 97%, and a $H_2$/CO ratio of 1.8. No carbonates or other new phases are observed after the long-term operation which indicates that PLNCG exhibits good chemical as well as phase stability under the POM reaction conditions. The spent membrane also maintains its compact dense structure except only a very thin Ni-enriched layer (around 5–10 μm) on the outer membrane surface resulting from the intimate contact with the catalyst, but without any negative effect on the membrane performance. To sum up, our hollow-fiber membrane reactor based on the alkaline-earth metal-free $CO_2$-tolerant PLNCG material exhibits promising stability in the POM with good performance in syngas production.

## Acknowledgments

The authors greatly acknowledge the financial support by National Science Fund for Distinguished Young Scholars of China (no. 21225625), the Sino-German Centre for Research Promotion (GZ676 and GZ911), and the Pearl River Scholar Program of Guangdong Province. Y. Wei is grateful for the financial support by Alexander von Humboldt Foundation. The authors also acknowledge F. Steinbach for technical support.

## Literature Cited

1. Hutchings GJ, Scurrell MS, Woodhouse JR. Oxidative coupling of methane using oxide catalysts. *Chem Soc Rev*. 1989;18:251–283.
2. Henrici-Olive G, Olive S. The Fischer-Tropsch synthesis: molecular weight distribution of primary products and reaction mechanism. *Angew Chem Int Ed Engl*. 1976;15:136–141.
3. Yang WS, Wang HH, Zhu XF, Lin LW. Development and application of oxygen permeable membrane in selective oxidation of light alkanes. *Top Catal*. 2005;35:155–167.

4. Bredesen R, Sogge J. In: The United Nations Economic Commission for Europe Seminar on Ecological Applications of Innovative Membrane Technology in Chemical Industry, Chem/Sem. 21/R. 12, 1–4 May 1996, Cetaro, Calabria, Italy.
5. Wang ZG, Kathiraser Y, Kawi S. High performance oxygen permeable membranes with Nb-doped $BaBi_{0.05}Co_{0.95}O_{3\text{-delta}}$ perovskite oxides. *J Membr Sci.* 2013;431:180–186.
6. Yang NT, Kathiraser Y, Kawi S. A new asymmetric $SrCo_{0.8}Fe_{0.1}Ga_{0.1}O_{3\text{-delta}}$ perovskite hollow fiber membrane for stable oxygen permeability under reducing condition. *J Membr Sci*. 2013;428:78–85.
7. Kathiraser Y, Wang ZG, Yang NT, Zahid S, Kawi S. Oxygen permeation and stability study of $La_{0.6}Sr_{0.4}Co_{0.8}Ga_{0.2}O_{3\text{-delta}}$ (LSCG) hollow fiber membrane with exposure to $CO_2$, $CH_4$ and He. *J Membr Sci*. 2013;427:240–249.
8. Zeng Y, Lin YS, Swartz SL. Perovskite-type ceramic membrane: synthesis, oxygen permeation and membrane reactor performance for oxidative coupling of methane. *J Membr Sci.* 1998;150:87–98.
9. Chen CS, Feng SJ, Ran S, Zhu DC, Liu W, Bouwmeester HJM. Conversion of methane to syngas by a membrane-based oxidation-reforming process. *Angew Chem Int Ed.* 2003;42:5196–5198.
10. Tsai CY, Dixon AG, Moser WR, Ma YH. Dense perovskite membrane reactor for partial oxidation of methane to syngas. *AIChE J*. 1997;43:2741–2750.
11. Yaremchenko AA, Valente AA, Kharton VV, Tsipis EV, Frade JR, Naumovich EN, Rocha J, Marques FMB. Oxidation of dry methane on the surface of oxygen ion-conducting membranes. *Catal Lett*. 2003;91:169–174.
12. Gu XH, Jin WQ, Chen CL, Xu NP, Shi J, Ma YH. YSZ-$SrCo_{0.4}Fe_{0.6}O_{3\text{-}\delta}$ membranes for the partial oxidation of methane to syngas. *AIChE J*. 2002;48:2051–2060.
13. Bouwmeester HJM. Dense ceramic membranes for methane conversion. *Catal Today*. 2003;82:141–150.
14. Balachandran U, Dusek JT, Maiya PS, Ma B, Mieville RL, Kleefisch MS, Udovich CA. Ceramic membrane reactor for converting methane to syngas. *Catal Today*. 1997;36:265–272.
15. Zeng PY, Ran R, Chen ZH, Gu HX, Shao ZP, Liu SM. Novel mixed conducting $SrSc_{0.05}Co_{0.95}O_{3\text{-}\delta}$ ceramic membrane for oxygen separation. *AIChE J*. 2007;53:3116–3126.
16. Pei S, Kleefisch MS, Kobylinski TP, Faber J, Udovich CA, Zhang-McCoy V, Dabrowski B, Balachandran U, Mieville RL, Poeppel RB. Failure mechanism of ceramic membrane reactor in partial oxidation of methane to synthesis gas. *Catal Lett*. 1994;30:201–212.
17. Wang HH, Feldhoff A, Caro J, Schiestel T, Werth S. Oxygen selective ceramic hollow fiber membranes for partial oxidation of methane. *AIChE J*. 2009;55:2657–2664.
18. Caro J, Schiestel T, Werth S, Wang HH, Kleinert A, Koelsch P. Perovskite hollow fiber membranes in the partial oxidation of methane to synthesis gas in a membrane reactor. *Desalination*. 2006;199:415–417.
19. Kleinert A, Feldhoff A, Schiestel T, Caro J. Novel hollow fiber membrane reactor for the partial oxidation of methane. *Catal Today*. 2006;118:44–51.
20. Tsai CY, Dixon AG, Moser WR, Ma YH, Pascucci MR. Dense perovskite, $La_{1\text{-}x}A'_xFe_{1\text{-}y}Co_yO_{3\text{-}\delta}$ (A' = Ba, Sr, Ca), membrane synthesis, applications and characterization. *J Am Ceram Soc*. 1998;81:1437–1444.
21. Luo HX, Efimov K, Jiang HQ, Feldhoff A, Wang HH, Caro J. $CO_2$-stable and cobalt-free dual-phase membrane for oxygen separation. *Angew Chem Int Ed*. 2011;50:759–763.
22. Zhu XF, Liu HY, Cong Y, Yang WS. Novel dual-phase membranes for $CO_2$ capture via an oxyfuel route. *Chem Commun.* 2012;48:251–253.
23. Yashima M, Sirikanda N, Ishihara T. Crystal structure, diffusion path, and oxygen permeability of a $Pr_2NiO_4$-based mixed conductor $(Pr_{0.9}La_{0.1})_2(Ni_{0.74}Cu_{0.21}Ga_{0.05})O4+\delta$. *J Am Chem Soc*. 2010;132:2385–2392.
24. Tang J, Wei YY, Zhou LY, Li Z, Wang HH. Oxygen permeation through a $CO_2$-tolerant mixed conducting oxide $(Pr_{0.9}La_{0.1})_2(Ni_{0.74}Cu_{0.21}Ga_{0.05})O_{4+\delta}$. *AIChE J*. 2012;58:2473–2478.
25. Wei YY, Tang J, Zhou LY, Xue J, Li Z, Wang HH. Oxygen separation through U-shaped hollow fiber membrane using pure $CO_2$ as sweep gas. *AIChE J*. 2012;58:2856–2864.
26. Hoang DL, Chan SH. Effect of reactor dimensions on the performance of an $O_2$ pump integrated partial oxidation reformer-a modelling approach. *Int J Hydrogen Energy*. 2006;31:1–12.
27. Wei YY, Liu HF, Xue J, Li Z, Wang HH. Preparation and oxygen permeation of U-shaped perovskite hollow fiber membranes. *AIChE J*. 2011;57:975–984.
28. Wei YY, Tang J, Zhou LY, Li Z, Wang HH. Oxygen permeation through U-shaped $K_2NiF_4$-type hollow fiber membranes. *Ind Eng Chem Res*. 2011;50:12727–12734.
29. Shao ZP, Yang WS, Cong Y, Dong H, Tong JH, Xiong GX. Investigation of the permeation behavior and stability of a $Ba_{0.5}Sr_{0.5}Co_{0.8}Fe_{0.2}O_{3\text{-}\delta}$ oxygen membrane. *J Membr Sci*. 2000;172:177–188.
30. Shao ZP, Haile SM. A high-performance cathode for the next generation of solid-oxide fuel cells. *Nature*. 2004;431:170–173.
31. Tong JH, Yang WS, Zhu BC, Cai R. Investigation of ideal zirconium-doped perovskite-type ceramic membrane materials for oxygen separation. *J Membr Sci*. 2002;203:175–189.
32. Tong JH, Yang WS, Cai R. Zhu BC, Lin LW. *Novel and ideal zirconium-based dense membrane reactors for partial oxidation of methane to syngas*. *Catal Lett*. 2002;78:129–137.
33. Dong H, Shao ZP, Xiong GX, Tong JH, Sheng SS, Yang WS. Investigation on POM reaction in a new perovskite membrane reactor. *Catal Today*. 2001;67:3–13.
34. Li QM, Zhu XF, He YF, Yang WS. Partial oxidation of methane in $BaCe_{0.1}Co_{0.4}Fe_{0.5}O_{3\text{-}\delta}$ membrane reactor. *Catal Today*. 2010;149:185–190.
35. Lu H, Tong JH, Cong Y, Yang WS. Partial oxidation of methane in $Ba_{0.5}Sr_{0.5}Co_{0.8}Fe_{0.2}O_{3\text{-}\delta}$ membrane reactor at high pressures. *Catal Today*. 2005;104:154–159.
36. Wang HH, Cong Y, Yang WS. Investigation on the partial oxidation of methane to syngas in a tubular $Ba_{0.5}Sr_{0.5}Co_{0.8}Fe_{0.2}O_{3\text{-}\delta}$ membrane reactor. *Catal Today*. 2003;82:157–166.
37. Luo HX, Wei YY, Jiang HQ, Yuan WH, Lv YX, Caro J, Wang HH. Performance of a ceramic membrane reactor with high oxygen flux Ta-containing perovskite for the partial oxidation of methane to syngas. *J Membr Sci*. 2010;350:154–160.
38. Gu XH, Yang L, Tan L, Jin WQ, Zhang LX, Xu NP. Modified operating mode for improving the lifetime of mixed-conducting ceramic membrane reactors in the POM environment. *Ind Eng Chem Res.* 2003;42:795–801.
39. Markov AA, Patrakeev MV, Leonidov IA, Kozhevnikov VL. Reaction control and long-term stability of partial methane oxidation over an oxygen membrane. *J Solid State Electrochem*. 2011;15:253–257.
40. Wang HH, Tablet C, Schiestel T, Werth S, Caro J. Partial oxidation of methane to syngas in a perovskite hollow fiber membrane reactor. *Catal Commun*. 2006;7:907–912.
41. Caro J, Caspary KJ, Hamel C, Hoting B, Koelsch P, Langanke B, Nassauer K, Noack M, Schiestel T, Schroeder M, Byun YC, Seidel-Morgenstern A, Tsotsas E, Voigt I, Wang HH, Warsitz R, Werth S, Aurel W. Catalytic membrane reactors for partial oxidation using perovskite hollow fiber membranes and for partial hydrogenation using a catalytic membrane reactor. *Ind Eng Chem Res*. 2007;46:2286–2294.
42. Wei YY, Huang L, Tang J, Zhou LY, Li Z, Wang HH. Syngas production in a novel perovskite membrane reactor with co-feed of $CO_2$. *Chin Chem Lett*. 2011;22:1492–1496.
43. Shao ZP, Dong H, Xiong GX, Yang WS. Syngas production using an oxygen-permeating membrane reactor with cofeed of methane and carbon dioxide. *Chin Chem Lett*. 2000;11:631–634.
44. Liu SL, Xiong GX, Dong H, Yang WS. Effect of carbon dioxide on the reaction performance of partial oxidation of methane over a LiLaNiO/g-$Al_2O_3$ catalyst. *Appl Catal*. 2000;202:141–146.

*Manuscript received Feb. 6, 2014, and revision received May 11, 2014.*